

Planetary waves: a numerical study of Rossby waves

Anna Lina P. Sjur and Jan-Adrian H. Kallmyr

December 14, 2018

Abstract

In this article, we solve the barotropic Rossby wave equation in the beta plane approximation for both bounded and periodic boundaries, using two different initial waves: a sine and gaussian. Numerically, we compare two implicit (centered) and explicit (forward) finite difference schemes. We study the stability and accuracy of both methods. From this analysis, we find that the centered scheme is stable to a higher time step Δt , and more accurate with a truncation error of order $\mathcal{O}(\Delta x^2)$. Using Hovmöller diagrams, we find that all our solutions propagate westward. For the sine wave, we can discern phase velocities: $v_p \approx -0.0063$ in the periodic domain (agreeing with the analytical value) and $v_p \approx -0.0050$ in the bounded domain. In two dimensions, we find that our solutions propagate only westward. This implies that the one-dimensional problem is a good representation of the two-dimensional problem.

1 Introduction

We encounter wave phenomena everywhere in the natural sciences. From quantum mechanics to oceanography, we find that be it the motion of a particle or the ocean, we require knowledge of wave-like behaviour to solve the problem. In quantum mechanics, a particle's wave function is described by a complex-valued diffusion equation, the Schrödinger equation, while in oceanography, we can describe ocean waves using the wave equation,

$$\frac{\partial^2 u}{\partial x^2} = \frac{\partial^2 u}{\partial t^2}, \quad (1)$$

where x and t denote the spatial and temporal coordinates, respectively. There exists many different equations describing waves. The Rossby wave equation (see Theory) will be the topic of this paper, in particular, we will model Rossby waves, first identified by Rossby (1939). These are inertial, planetary waves in the Earth's atmosphere and ocean which motions contribute to extreme weather (Mann

et al., 2017), might drive the El-Niño southern oscillation (ENSO) (Bosc and Delcroix, 2008), and is also produced by ENSO, see Battisti (1989). While we hope the reader appreciate the wide range of phenomena related to these waves, our article presents a numerical study of the waves isolated from other processes. We therefore begin by describing fundamental theory of waves and partial differential equations in the Theory section, present our algorithm and the technicalities relating to its implementation. In the Results section, we present our data as figures, before discussing their implications in the Discussion section. Concluding our paper, we present our final thoughts on the topic of simulating Rossby waves.

2 Theory

2.1 Wave analysis

Waves are solutions of the wave equation (see eq. 1), and have certain properties such as the

phase velocity

$$c = \frac{\lambda}{T} = \frac{\omega}{k}, \quad (2)$$

where λ is the wavelength, T the period, ω the angular frequency and k the wavenumber. We found the phase velocity of a variety of waves graphically by studying Hovmöller diagrams (Hovmöller, 1949).

2.2 Rossby wave equation

Rossby waves are low frequency waves induced by the meridional variation of the Coriolis parameter f . This parameter depends on the rotation of the Earth Ω and the latitude φ , and is given by

$$f = \Omega \sin \varphi. \quad (3)$$

An approximation where f is set to vary linear in space is called the β -plane approximation, and can be written as

$$f = f_0 + \beta y, \quad (4)$$

where $\beta = \left. \frac{df}{dy} \right|_{\varphi_0} = \frac{2\Omega}{a} \cos \varphi_0$, a being the radius of the Earth. Combining the β -plane approximation with the shallow water vorticity equation, you get the quasi-geostrophic vorticity equation. This can be linearised, and by assuming a constant mean flow without bottom topography, you get the barotropic Rossby wave equation:

$$(\partial_t + U \partial_x) \nabla_H \psi + \beta \partial_x \psi = 0. \quad (5)$$

Here, ψ is the stream function describing the velocity perturbation, ∂_x denotes $\frac{\partial}{\partial x}$, ∇_H is the horizontal divergence $\partial_x + \partial_y$ and U is the mean velocity. In this report, we will assume no mean velocity, i.e. $U = 0$, in which case equation (5) simplifies to

$$\partial_t \nabla_H \psi + \beta \partial_x \psi = 0. \quad (6)$$

Two forms of boundaries will be examined in this report, that is periodic and constant

boundaries. The first case can be used to describe an atmosphere that wraps around the earth, where the stream function is equal at the end-points. The latter case, where the stream function has a constant value at the boundaries, can be used to describe an ocean basin.

When extending the problem to two dimensions, we require that the stream function is constant at all boundaries for the bounded case. For the periodic case, the stream function should wrap around in the east-west direction, which corresponds to the x -direction, while being constant at the north and south boundaries, corresponding to the boundaries in the y -direction.

A possible solution to (6) in one dimension with periodic boundaries, where $x \in [0, L]$, is given by

$$\psi = A \cos(kx - \omega t), \quad (7)$$

where $k = \frac{2n\pi}{L}$ and $\omega = -\frac{\beta L}{2n\pi}$. The phase speed c can be calculated through the dispersion relation, given by

$$c = \frac{\omega L}{2n\pi} = -\beta \left(\frac{L}{2n\pi} \right)^2. \quad (8)$$

Since β is positive for all latitudes, the phase speed will be negative, implying that Rossby waves travels from east to west in a bounded domain.

The same problem, but with constant boundaries equal to zero, has the possible solution

$$\psi = A \sin\left(\frac{\pi n}{L}x\right) \cos(kx - \omega t), \quad (9)$$

with $k = \frac{L}{\pi n}$ and $\omega = -\frac{\beta}{2k}$. Here, the phase speed is given by

$$c = \frac{\omega L}{2n\pi} = -\frac{\beta}{4} \quad (10)$$

Again, the phase speed is negative. Equation (9) describes a cosine wave where the amplitude is dependent on the position, following a sine curve with zeros at the boundaries.

2.3 Discretisation and algorithm

Scaling eq. 6, we essentially wanted to solve two equations

$$\partial_t \zeta + \partial_x \psi = 0 \quad (11)$$

$$\nabla_H \psi = \zeta, \quad (12)$$

where the latter is Poisson's equation. In one dimension, equation (12) simplifies to

$$\partial_{xx} \psi = \zeta, \quad (13)$$

To discretise, we use the following schemes:

$$\partial_q f \approx \frac{f_{q+1} - f_q}{\Delta q}, \quad (14)$$

$$\partial_q f \approx \frac{f_{q+1} - f_{q-1}}{2\Delta q}, \quad (15)$$

$$\partial_{qq} f \approx \frac{f_{q+1} - 2f_q + f_{q-1}}{(\Delta q)^2}, \quad (16)$$

where f is arbitrary and q a general coordinate. Here eq. 14 is the explicit forward scheme, with a truncation error proportional to Δq , and eq. 15 the implicit centered scheme, with a truncation error proportional to Δq^2 . Equation (16) does as well have a truncation error proportional to Δq^2 . Letting $t^n = n\Delta t$ and $x_j = j\Delta x$, eq. 11 becomes

$$\zeta_j^{n+1} = \zeta_j^n - \frac{\Delta t}{2\Delta x} (\psi_{j+1}^n - \psi_{j-1}^n) \quad (17)$$

in the explicit scheme, and

$$\zeta_j^{n+1} = \zeta_j^{n-1} - \frac{\Delta t}{\Delta x} (\psi_{j+1}^n - \psi_{j-1}^n) \quad (18)$$

in the implicit scheme. For Poisson's equation, we simply have

$$\frac{\psi_{j+1}^{n+1} - 2\psi_j^{n+1} + \psi_{j-1}^{n+1}}{(\Delta x)^2} = \zeta_j^{n+1}. \quad (19)$$

for one dimension. Our general algorithm is then Algorithm 1. What remains now is to de-

```

initialise  $\psi^0, \zeta^0$ ;
for  $n = 0, 1, \dots, T$  do
    for  $j = 0, 1, \dots, X$  do
        solve for  $\zeta_j^{n+1}$  using explicit or
        implicit scheme;
    solve for  $\psi^{n+1}$  using Gaussian
    eliminatin or Jacobi's method;

```

Algorithm 1: Algorithm for solving the 1+1 dimensional Rossby wave equation. Here T and X are the grid sizes in the temporal and spatial dimensions respectively.

termine how to solve the equations for closed and periodic boundary conditions. In the case of closed boundaries we had the Dirichlet boundary conditions, and could use gaussian elimination as outlined in one of our earlier papers (Sjur and Kallmyr, 2018). As for the periodic domain, we found that the resulting matrix form of the Laplacian would be singular. This prompted us to implement Jacobi's method, as described by Hjorth-Jensen (2015).

Jacobi's method is an iterative method, involving making a guess for ψ_j^{n+1} for all j , and then, by rearranging Poisson's equation, calculating ψ_j^{n+1} . The stream function is recalculated until the difference in ψ between two iterations is essentially zero.

Up until this point we had only considered the 1 + 1 dimensional Rossby wave. Expanding to 2 + 1 involves solving equation (12) using Jacobis method. Discretising, the Poisson equation in two dimensions becomes

$$\frac{\psi_{i,j+1}^{n+1} + \psi_{i+1,j}^{n+1} - 4\psi_{i,j}^{n+1} + \psi_{i,j-1}^{n+1} + \psi_{i-1,j}^{n+1}}{(\Delta x)^2} = \zeta_{i,j}^{n+1}, \quad (20)$$

given that $\Delta x = \Delta y$. Algorithm REF outlines the algorithm for solving the two-dimensional case.

```

initialise  $\psi^0, \zeta^0$ ;
for  $n = 0, 1, \dots, T$  do
    for  $j = 0, 1, \dots, Y$  do
        for  $i = 0, 1, \dots, X$  do
            solve for  $\zeta_{i,j}^{n+1}$  using explicit
            or implicit scheme;
        solve for  $\psi^{n+1}$  using Jacobi's
        method;

```

Algorithm 2: Algorithm for solving the 2+1 dimensional Rossby wave equation. Here T , X and Y are the grid sizes in the temporal and spatial dimensions respectively.

Simulating the ocean, we chose a bounded domain in both directions, while for the atmosphere it made sense to keep the domain closed zonally, and periodic meridionally.

It should be noted that due to time constraints, the code used to generate the data shown in Figure 8 does not handle the eastward boundary correctly.

2.4 Implementation

We implemented our algorithms in C++ using the `armadillo` and `LAPACK` libraries to handle matrix operations. To analyse data and produce figures, we used python 3.6 with a standard set of modules: `matplotlib`, `numpy` and `seaborn`. All our code and figures can be found in a github repository ¹.

3 Results

Shown in Figure 1 is the breakdown of the forward difference scheme at around $\Delta t = 1$. We see that the centered difference scheme remains relatively stable, while the forward

scheme wave increases in amplitude over time, showing instability.

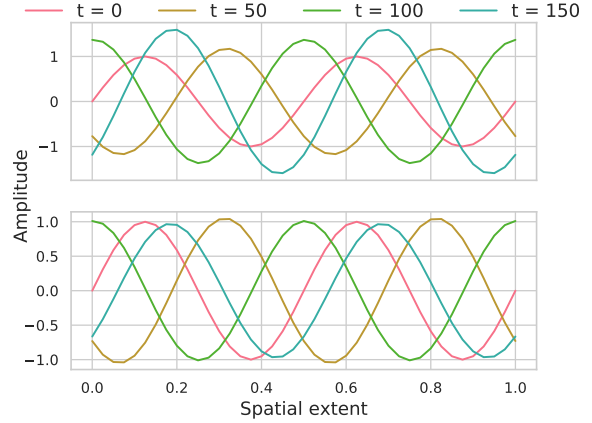


Figure 1: Comparison between the explicit forward difference scheme (top) and the implicit centered difference scheme (bottom) for $\Delta t = 1$.

Looking at Figure 2, we observe the time evolution of a sine wave in the periodic domain. We see that the wave is easterly (traveling towards the west). There are four distinct anti-nodes throughout the entire duration of the wave, and a phase velocity is determined to be $v_p \approx 0.0063$. After a time $t = 80$ we can see that the wave is in phase to its initial state.

Considering now the bounded sine wave (Figure 3), the direction of propagation is still west. The shape of the curve appears to be the same as for the periodic case, except that the equilibrium line of the sine curve is shifting up and down, so that the boundary conditions are satisfied. Here we determine a phase velocity, $vp \approx 0.005$.

From Figure 4, 5 and 6, we see that, in general, the periodic gaussian wave exhibits different behaviour compared to the sine wave. There are at most two distinct anti-nodes at any point in time, and there looks to be a changing pattern in time, compared to the sine

¹<https://github.com/janadr/FYS3150/tree/master/prosjekt5>

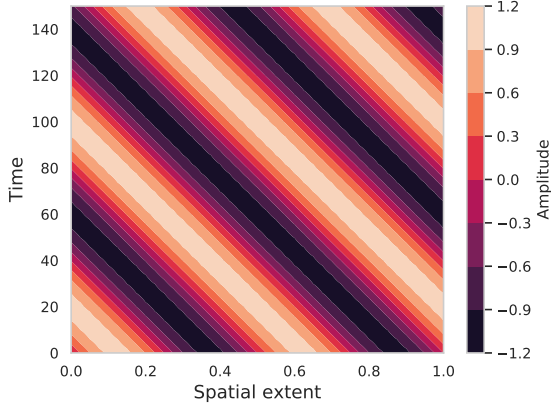


Figure 2: Hovmöller diagram of a Rossby wave with **periodic** boundary conditions, initially a sine wave using a implicit scheme, where $\Delta x = 0.025$ and $\Delta t = 0.1$.

waves which always look the same. For varying width, σ , we see that the location of the anti-node are more concentrated in the middle for lower σ (Figure 4) and more spread out for higher σ (Figure 6).

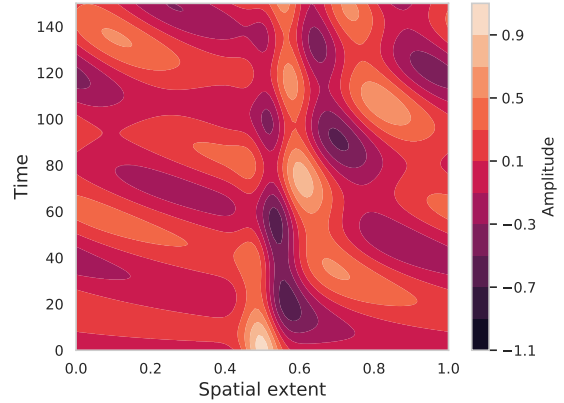


Figure 4: Hovmöller diagram of a Rossby wave with **periodic** boundary conditions, initially a centered gaussian ($x_0 = 0.5$) using a implicit scheme. Here $\sigma = 0.05$, $\Delta x = 0.01$ and $\Delta t = 0.1$.

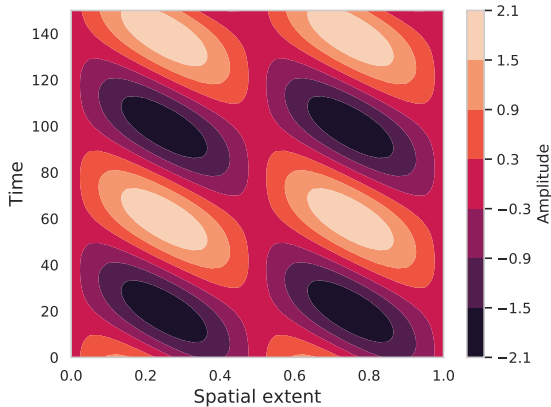


Figure 3: Hovmöller diagram of a **bounded** Rossby wave with a initial sine wave using a implicit scheme. Here $\Delta x = 0.025$ and $\Delta t = 0.1$.

In Figure 7 we show the Hovmöller diagram of a gaussian with closed boundaries. In this case, while there are still variations in time, we can clearly discern oscillations between minima and maxima.

Figure 9 and 8 shows the evolution of an initial product between two sine waves, one in the x-direction and one in the y-direction, resulting in an two dimensional wave, for four different time steps, both in a periodic and bounded domain. In the periodic domain, the wave seems to keep its structure, while shifting in the x-direction.

For the bounded two dimensional domain, the amplitude of the wave have decreased closer to the x-boundaries for the time steps $t \neq 0$.

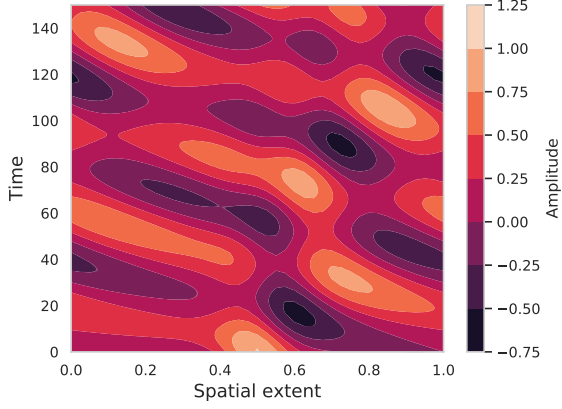


Figure 5: Hovmöller diagram of a Rossby wave with **periodic** boundary conditions, initially a centered gaussian ($x_0 = 0.5$) using a implicit scheme. Here $\sigma = 0.1$, $\Delta x = 0.025$ and $\Delta t = 0.1$.

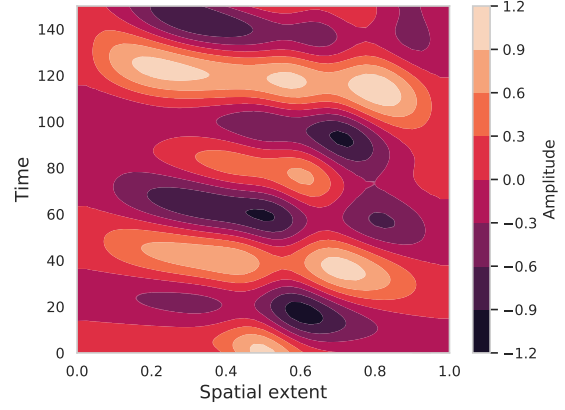


Figure 7: Hovmöller diagram of a **bounded** Rossby wave initially a centered gaussian ($x_0 = 0.5$) using a implicit scheme. Here $\sigma = 0.1$, $\Delta x = 0.025$ and $\Delta t = 0.1$.

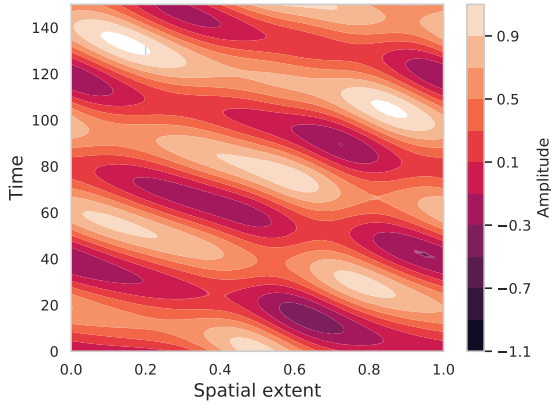


Figure 6: Hovmöller diagram of a Rossby wave with **periodic** boundary conditions, initially a centered gaussian ($x_0 = 0.5$) using a implicit scheme. Here $\sigma = 0.15$, $\Delta x = 0.025$ and $\Delta t = 0.1$.

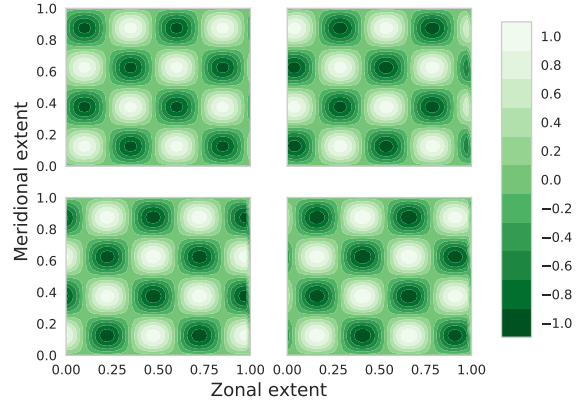


Figure 8: 2+1 dimensional time evolution of a sine wave in the **periodic** domain, where time advances from left to right, top to bottom, for $t = 0, 50, 100, 150$ respectively. Here $\Delta x = 0.025$ and $\Delta t = 0.1$

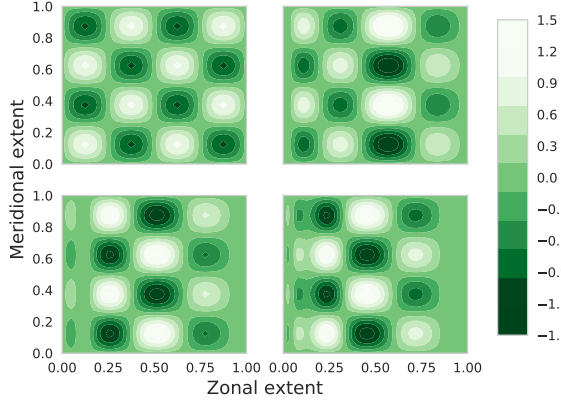


Figure 9: 2+1 dimensional time evolution of a sine wave in the **bounded** domain, where time advances from left to right, top to bottom, for $t = 0, 50, 100, 150$ respectively. Here $\Delta x = 0.025$ and $\Delta t = 0.1$

4 Discussion

A deeper analysis could be performed for measuring the stability criterion for the two schemes. Figure 1 only shows a snapshot where the explicit schemes fails. A more critical analysis would require finding the stability as a function of Δt .

Looking back at the Hovmöller diagrams, we find that Figure 2 corresponds well with the analytical expression in eq. 7 as shown in the figure is the very distinct Hovmöller diagram for a cosine wave with a constant amplitude of 1. In the bounded case (Figure 3) we find that the amplitude still is 1, compared to the equilibrium line. Here, the numerical solution does not match the analytical solution. The bounded solution with an initial Gaussian wave, however, seems to match better with the analytical solution, since the amplitude increases toward the centre of the domain. The Gaussian initial wave does, on the other hand, not match well with the analytical periodic solution. This leads to the impression that an

initial sine wave is better for the periodic domain, while a Gaussian wave is preferred for the bounded domain. Both waves are east-erlies, which is as expected from the analytical negative dispersion relation (eq. 10), and correlates with Rossby’s original observations (Rossby, 1939).

As for the gaussian waves, we have no analytical solutions, but find that they still propagate westward (as seen in Figure 5 and 7). The results we see for varying σ implies that the distribution of anti-nodes of the gaussian wave is preserved throughout the motion, seeing as they become more concentrated for a narrower wave, and less concentrated for a wider wave. While we couldn’t find the phase velocity, we can qualitatively (and very roughly) see that the phase velocity seem to decrease in the bounded domain, which is consistent with the sine wave.

In two dimensions we only present the sine waves, as the gaussian waves yielded unphysical results. From Figure 8 and 9 we could not discern the direction of propagation. However, referring to the code for animating the time evolution found in the GitHub repository (see Theory), it can be seen that the wave is travelling to the west. This being the case for both types of boundary conditions indicates that the one-dimensional problem is a representation for the two-dimensional problem, as there is very little, if no movement zonally.

5 Conclusion

We solved the barotropic Rossby wave equation in the betaplane approximation (6) for periodic and bounded boundaries.

Numerically, we found a implicit centered difference scheme to be most accurate and stable, compared with a explicit forward difference scheme. We therefore used the implicit method throughout the paper.

In the one-dimensional case we find agreement between the analytical and numerical solutions of a sine wave in both domains. For both boundaries, the waves propagate towards the west, which is in agreement with our analytical dispersion relation and the established literature. We also calculated a value of the phase velocity in both cases, which are in agreement with our analytical phase velocity.

For the gaussian waves, we had no analytical solution, but observed our numerical solutions to be waves moving west in both domains. No phase velocity could be discerned from the Hovmöller diagrams.

In the two-dimensional case, we considering two boundary-value problems. Simulating the ocean, we chose all four boundaries to be closed, representing the continents. Simulating the atmosphere, we chose closed boundaries in the meridional and periodic boundaries in the zonal. We found that the one-dimensional case was a good representation of the problem, as the waves propagate only zonally in the two-dimensional problem as well.

References

- David S Battisti. On the role of off-equatorial oceanic rossby waves during enso. *Journal of physical Oceanography*, 19(4):551–560, 1989.
- Christelle Bosc and Thierry Delcroix. Observed equatorial rossby waves and enso-related warm water volume changes in the equatorial pacific ocean. *Journal of Geophysical Research: Oceans*, 113(C6), 2008.
- Morten Hjorth-Jensen. Computational physics. <https://github.com/CompPhysics/ComputationalPhysics/blob/master/doc/Lectures/lectures2015.pdf>, 2015.
- Ernest Hovmöller. The trough-and-ridge diagram. *Tellus*, 1(2):62–66, 1949.
- Michael E Mann, Stefan Rahmstorf, Kai Kornhuber, Byron A Steinman, Sonya K Miller, and Dim Coumou. Influence of anthropogenic climate change on planetary wave resonance and extreme weather events. *Scientific Reports*, 7:45242, 2017.
- Carl-Gustaf Rossby. Relation between variations in the intensity of the zonal circulation of the atmosphere and the displacements of the semi-permanent centers of action. *J. Mar. Res.*, 2:38–55, 1939.
- Anna Lina P. Sjur and Jan-Adrian H. Kallmyr. Two methods of solving linear second-order differential equations. <https://github.com/janadr/FYS3150/blob/master/prosjekt1/tex/main.pdf>, 2018.